Validation of Remotely Sensed XCO_2 Products With TCCON Observations in East Asia

Meng Ji, Yongming Xu, Yang Zhang, Yaping Mo, Shanyou Zhu, Wei Wang, Minqiang Zhou, Isamu Morino, Hirofumi Ohyama, Kei Shiomi, and Young-Suk Oh

***Abstract*—As an important greenhouse gas (GHG) in the atmosphere, carbon dioxide (CO_2) has a great impact on global climate change. Accurate knowledge of the spatiotemporal variations of CO_2 is of great significance for understanding the carbon cycle and evaluating the effectiveness of carbon emission reduction. In recent years, several satellites with CO_2 sensors have been launched and a series of atmospheric CO_2 concentration products have been developed using different retrieval algorithms. This study validated nine satellite XCO_2 products derived from Greenhouse gases Observing SATellite (GOSAT), GOSAT-2, Orbiting Carbon Observatory-2 (OCO-2), and OCO-3: including ACOS-GOSAT, NIES-GOSAT, BESD-GOSAT, OCFP-GOSAT, SRFP-GOSAT, EMMA, GOSAT-2, OCO-2, and OCO-3 XCO_2. The remotely sensed XCO_2 products were compared with the XCO_2 observations from six Total Carbon Column Observing Network (TCCON) stations in East Asia for validation. The results showed that the OCO-2 XCO_2 product outperformed other products, with the highest R^2 of 0.94 and the lowest MAE of 1.24 ppm. The ACOS-GOSAT and EMMA-GOSAT XCO_2 products also showed favorable accuracies, both achieving R^2 of 0.93 and corresponding MAE values of 1.29 and 1.31 ppm, respectively. The GOSAT-2 XCO_2 product showed the poorest accuracy, with an R^2 of 0.77 and a mean absolute error of 3.28 ppm. There was a significant overestimation of the bias-uncorrected GOSAT-2 XCO_2 product in East Asia, and it indicated that bias correction must be performed for this XCO_2 product. The accuracy of TCCON XCO_2 was not consistent with remotely sensed XCO_2 at different stations. The RJ, JS, AN, and TK TCCON stations generally showed better agreements between satellite estimates and TCCON observations, except for the GOSAT-2 XCO_2 product.**

***Index Terms*—Greenhouse gases Observing SATellite (GOSAT), GOSAT-2, Orbiting Carbon Observatory-2 (OCO-2), OCO-3, Total Carbon Column Observing Network (TCCON), validation, XCO_2 product.**

I. Introduction

Since the Industrial Revolution, the combustion of fossil fuels and other human activities have emitted large amounts of greenhouse gases (GHGs) into the atmosphere [1], [2]. As the most dominant GHG, CO_2 has increased substantially, with the concentration rising from 280 ppm in 1760 to 410 ppm in 2020 [3]. The increase in the concentration of CO_2 and other GHGs enhances the thermal insulating effect of the atmosphere [4], [5], [6], which has in turn exacerbated global warming [7], [8]. Global warming has led to a series of environmental alterations, including the rise in sea level, the decrease in freshwater resources, the increase of extreme weather, and the intensification of the spread of diseases [9], [10], [11], [12], [13]. These consequences eventually impact human life, society, and national security [14], [15]. The problem of carbon dioxide emission has attracted the attention of various countries [16]. China announced the goal of achieving emissions by 2030 and carbon neutrality by 2060, adhering to the path of ecological priority, green and low-carbon development [17], [18]. Accurate knowledge of the spatial and temporal variations of atmospheric CO_2 concentrations provides important data support for formulating carbon emission reduction policies, and therefore is of great significance for promoting carbon peaking and carbon neutrality targets.

Traditional ground-based observation has high accuracy and reliability. However, due to the high prices and maintenance costs of instruments at ground observation stations, the global count of effective ground stations is limited and their spatial distribution is uneven. The station observations cannot obtain atmospheric CO_2 concentrations over large areas. Satellite remote sensing has the advantages of expansive coverage, continuity, and low cost, which provides an alternative to ground observation. Recently, several remote sensing satellites that carried specialized CO_2 sensors have been launched, including SCIAMACHY, Greenhouse gases Observing SATellite (GOSAT),

Manuscript received 19 November 2023; revised 25 February 2024; accepted 1 March 2024. Date of publication 19 March 2024; date of current version 1 April 2024. This work was supported in part by the Xinjiang Production and Construction Corps Science and Technology Tackling Program in Priority Areas (2022AB016), in part by the Shihezi City Science and Technology Tackling Program in Priority Areas (2022NY03), in part by the Korea Meteorological Administration Research and Development Program "Development of Integrated Climate Change Monitoring and Analysis Techniques" under Grant KMA2018-00324, and in part by the Xianghe site is supported by the National Key Research and Development Program of China (2023YFB3907505). *(Corresponding author: Yongming Xu.)*

Meng Ji, Yongming Xu, Yang Zhang, Yaping Mo, and Shanyou Zhu are with the School of Remote Sensing and Geomatics Engineering, Nanjing University of Information Science and Technology, Nanjing 210044, China (e-mail: jm026@nuist.edu.cn; xym30@263.cn; 20211211035@nuist.edu.cn; yaping.mo@port.ac.uk; zsyzgx@163.com).

Wei Wang is with the Key Laboratory of Environmental Optics and Technology, Anhui Institute of Optics and Fine Mechanics, Hefei 230031, China (e-mail: wwang@aiofm.ac.cn).

Minqiang Zhou is with the CNRC, Institute of Atmospheric Physics, Chinese Academy of Sciences, Beijing 100029, China (e-mail: minqiang.zhou@mail.iap.ac.cn).

Isamu Morino and Hirofumi Ohyama are with the Earth System Division, National Institute for Environmental Studies, Tsukuba 305-0053, Japan (e-mail: morino@nies.go.jp; oyama.hirofumi@nies.go.jp).

Kei Shiomi is with the Japan Aerospace Exploration Agency, Tsukuba 305-0047, Japan (e-mail: shiomi.kei@jaxa.jp).

Young-Suk Oh is with the Climate Research Department, National Institute of Meteorological Sciences, Seogwipo 63568, South Korea (e-mail: ysoh306@gmail.com).

Digital Object Identifier 10.1109/JSTARS.2024.3378229

GOSAT-2, OCO-2, OCO-3, and TanSat, and different algorithms have also been developed to retrieve the atmospheric CO_2 column concentration (XCO_2) from remote sensing data. To date, a lot of remotely sensed XCO_2 products have been released. Due to the different sensors and algorithms, different XCO_2 products have different accuracies. To verify the reliability of satellite XCO_2 products, several scholars have carried out relevant studies on the validation of XCO_2 products using ground measurements as reference. Zhang et al. [19] validated the BESD-SCIAMACHY XCO_2 products, the National Institute for Environmental Studies-GOSAT (NIES-GOSAT) XCO_2 products, and the Atmospheric CO_2 Observations from Space-GOSAT (ACOS-GOSAT) XCO_2 products using observations from seven TCCON stations in the northern hemisphere. The results showed that the correlation coefficients between the three XCO_2 products and the TCCON site data were 0.64, 0.82, and 0.76, respectively, and the error standard deviations were 2.91, 2.27, and 2.26 ppm, respectively. Liang et al. [20] validated the GOSAT and OCO-2 products using the global TCCON observation network and found that the error standard deviation between GOSAT XCO_2 and TCCON XCO_2 was 2.22 ppm, the error standard deviation between OCO-2 XCO_2 and TCCON XCO_2 was 1.56 ppm, and the XCO_2 values of the OCO-2 product were 1.77 ppm higher on average than those of the GOSAT product. Zhang et al. [21] validated the OCO-2 XCO_2 product from 2015 to 2018 using the global TCCON observation network and found that the mean absolute error between the OCO-2 derived and TCCON observed XCO_2 was 0.25 ppm, and the root mean square error was 1.14 ppm. Wunch et al. [22] validated the OCO-2 XCO_2 product from 2014 to 2017 using the observations of 19 TCCON stations and found that the OCO-2 XCO_2 product had an absolute median bias of less than 0.4 ppm. Meng et al. [23] validated the GOSAT XCO_2 product from 2009 to 2017 using 18 TCCON stations around the world. The results showed that the average deviations between the GOSAT derived and TCCON observed XCO_2 in the four subregions of North America, East Asia, Europe, and Oceania were 2.19 ± 2.19, 2.23 ± 2.69, 2.01 ± 2.49, and 1.59 ± 1.79 ppm, respectively. The highest agreement between them was observed in the region between 0° and 30° S, with a standard deviation of 1.57 ppm and a correlation coefficient of 0.94. Fang et al. [24] validated the ACOS-GOSAT, OCO-2, and Tansat XCO_2 products using 26 TCCON stations around the world. They indicated that Tansat XCO_2 had the highest accuracy with an R^2 of 0.88 and an RMSE of 1.06 ppm, followed by OCO-2 XCO_2 with an R^2 of 0.82 and an RMSE of 1.07 ppm, and ACOS-GOSAT XCO_2 had the lowest accuracy with an R^2 of 0.81 and an RMSE of 1.23 ppm. Zheng et al. [25] validated the OCO-2 XCO_2 product from September 2014 to February 2022 and the ACOS-GOSAT XCO_2 product from April 2009 to May 2016 using 20 TCCON stations and found that OCO-2 and ACOS-GOSAT XCO_2 products showed a strong correlation with TCCON XCO_2 with R^2 of 0.91 and 0.85, respectively. Karbasi et al. [26] validated the GOSAT XCO_2 product retrieved by ACOS, NIES, and SRFP algorithms from 2009 to 2021 using eight TCCON stations. The results showed that the mean correlation coefficients between the retrieved XCO_2 of these the three algorithms and the station observations ranged from 0.14 to 0.98, 0.11 to 0.97, and 0.10 to 0.95, respectively, and the standard deviations ranged from 1.08 to 4.7 ppm, 1.13 to 4.3 ppm, and 1.48 to 24.6 ppm, respectively. Expect Fang and Zheng's studies used the new version of TCCON XCO_2 data (GGG2020) as reference data, other studies used the old GGG2014 version. These studies primarily validated the XCO_2 products of a specific satellite platform. There is a lack of comprehensive comparison and validation of the XCO_2 products derived from various sensors and algorithms. Furthermore, most studies were carried out on a global or hemispheric scale. However, due to the differences in human activities and surface characteristics, the reliability of XCO_2 products is also different in different regions.

With a large population and rapid economic development, East Asia plays an important role in the global carbon cycle. This study aims to verify the nine existing XCO_2 products in East Asia using the observations from six TCCON stations. The validation results can provide comprehensive information on the reliability of XCO_2 products in this area, and provide valuable reference for the carbon reduction strategies of East Asian countries, especially China.

II. Sensors and Data

A. Satellite XCO_2 Data

Nine XCO_2 products derived from four platforms (GOSAT, GOSAT-2, OCO-2, and OCO-3) were selected for validation in this study, including ACOS-GOSAT, NIES- GOSAT, Bremen Optimal Estimation-DOAS-GOSAT (BESD-GOSAT), the University of Leicester full-physics XCO_2-GOSAT (OCFP-GOSAT), the RemoTeC XCO_2 Full Physics-GOSAT (SRFP-GOSAT), and the ensemble median algorithm (EMMA-GOSAT, GOSAT-2, OCO-2, and OCO-3). Among them, five products were derived from GOSAT data using different algorithms, three products were derived from GOSAT-2, OCO-2, and OCO-3, respectively, and the EMMA product was produced by assembling several available XCO_2 products. Table I outlines the data version and date range in this study.

GOSAT, launched by the Japan Aerospace Exploration Agency (JAXA) in January 2009, is the world's first satellite for monitoring GHGs [27]. The satellite carries a Thermal and Near-infrared Sensor for Carbon Observation (TANSO), which consists of a Fourier transform spectrometer (FTS) and a Cloud and Aerosol Imager (CAI). TANSO-FTS is the satellite's main sensor for observing GHGs, which was three short-wave infrared bands and one broad thermal infrared band, with a spatial resolution of 10.5 km and a revisit period of 3 days. It has a swath width of 1000 km, with five observation points (footprints) until July 31, 2010, and three observation points since August 1, 2010, in the cross-track direction under the regular observation model.

The NIES-GOSAT XCO_2 product was developed by Japan's National Institute for Environmental Studies using the NIES algorithm. This algorithm utilized the widely-used optimal estimation method that reflects the difference between the simulated and observed radiation on the state variables by repeating the radiative transfer model simulated radiation as well

TABLE I
SATELLITE XCO_2 DATA USED IN THIS STUDY

Satellite	Algorithm	Version	Temporal coverage
GOSAT	NIES	v03.05	2011.07.28-2022.06.30
	ACOS	ACOS_L2_Lite_FP v9r	2011.07.28-2020.06.30
	BESD	v01.00.02	2014.04.01-2021.12.31
	OCFP	v7.3	2011.07.28-2021.12.31
	SRFP	v2.3.8	2011.07.28-2020.06.29
GOSAT-2	NIES	v02.00	2019.03.01-2022.12.31
OCO-2	ACOS	OCO_2_L2_Lite_FP v10r	2014.09.06-2022.02.28
OCO-3	ACOS	OCO3_L2_Lite_FP v10.4	2019.08.06-2022.12.31
Ensemble	EMMA	v4.3	2011.07.28-2020.06.30

as the Levenberg–Marquardt equations to obtain the optimal state variables [28]. The NIES product is the standard GOSAT XCO_2 product. However, several instructions also developed retrieval algorithms to generate XCO_2 products. The National Aeronautics and Space Administration (NASA) proposed the ACOS algorithm [29], [30], the University of Bremen developed the BESD algorithm [31], [32], and the University of Leicester developed the OCFP algorithm [33], and The Netherlands Institute for Space Research developed SRFP algorithm [26], [34], [35]. These algorithms are also based on the optimal estimation method, but employ different data screen schemes, priori information, aerosol models, and bias correction methods [36].

GOSAT-2, launched in October 2018, is the follow-up project of GOSAT. The TANSO-2 on board consists of FTS-2 and CAI-2 [37]. Compared with FTS, FTS-2 has higher signal-to-noise ratios in the short-wave infrared and thermal infrared bands, which not only improves detection accuracy but also allows the acquisition of atmospheric concentration data at higher latitudes in the northern hemisphere. Moreover, FTS-2 incorporates an Intelligent Pointing (IP) technology to collect more useful data under cloudy weather. Compared with CAI, CAI-2 has three new bands, which can be used for both forward and backward-looking observations, allowing cloud identification in all directions [38]. The GOSAT-2 data have a spatial resolution of 9.7 km and a 6-day revisit period. The GOSAT-2 XCO_2 product is produced by Japan's National Institute for Environmental Studies using the NIES retrieval algorithm. The GOSAT-2 XCO_2 product of v02.00 is bias uncorrected. However, empirical bias corrected coefficients are provided [39].

OCO-2, which was launched by NASA in July 2014, is the world's second satellite for tracking GHGs from space after GOSAT. It carries a three-channel high-resolution grating spectrometer that measures sunlight scattered and reflected radiation from the land surface or atmosphere from near-infrared to short-wave infrared bands [40]. It has a spatial resolution of 2.25 km × 1.29 km, which is much higher than GOSAT, and therefore, can collect many more cloud-free pixels. Its swath width is 10 km with eight across-track measurements. The revisit period is 16 days. The OCO-2 XCO_2 product is retrieved by NASA using the ACOS algorithm.

OCO-3 was launched by NASA in March 2019. It is mounted on the exterior of the Japanese Experiment Module-Exposure Facility module of the International Space Station. It carries the same three-channel high-resolution grating spectrometer on OCO-2. However, due to the different orbit of the International Space Station, the revisit period varies from 0 to multiple per day. The OCO-3 XCO_2 product is also retrieved by NASA using the ACOS algorithm.

In addition, there is an ensemble XCO_2 product that was generated by the ensemble median algorithm (EMMA). It combines ten XCO_2 products derived from SCIAMACHY, OCO-2, GOSAT, and GOSAT-2 by calculating the median over a spatial range of 10° × 10° to produce the final XCO_2 values. The ensemble method is effective in reducing biases as well as occasional outliers [41], [42].

Among the abovementioned XCO_2 products, ACOS-GOSAT, OCFP-GOSAT, SRFP-GOSAT, EMMA-GOSAT, GOSAT-2, OCO-2, and OCO-3 XCO_2 products contain quality control flag information (XCO_2_quality_flag). Flag value of "xco_2_quality_flag = 0" denotes good quality. In this study, only the pixel values with high quality were selected for validation.

B. TCCON XCO_2 Data

Total Carbon Column Observing Network (TCCON) is a global ground-based network to observe the amount of CO_2, CO, N_2O, CH_4, and other trace gases in the atmosphere. The main measurement instrument at each TCCON station is the Bruker IFS 125HR Fourier transform spectrometer. The spectrometer measures the absorption of atmospheric trace gases into direct sunlight mainly in the near-infrared band, and accurately retrieves the total column concentration of the gases based on a nonlinear least-squares spectral fitting algorithm [43]. Under clear-sky or low-cloud conditions, the spectrometer has a measurement accuracy of 0.25%.

TCCON provides independent measurements to validate the atmospheric CO_2 column concentration derived from satellite remote sensing data [44], [45], [46]. To minimize the inconsistency between different TCCON stations due to differences in retrieval methods, the same GGG and GFIT retrieval software is employed to retrieve the data for all stations. Thirty three TCCON stations across the world officially provide XCO_2 observation data. In this study, XCO_2 data from six TCCON stations in East Asia are used: Heifei (HF), Xianghe (XH),

TABLE II
INFORMATION OF THE SIX TCCON STATIONS IN EAST ASIA USED FOR VALIDATION

Station	Abbreviation	country	Longitude (°)	Latitude (°)	Temporal coverage	Reference
Hefei	HF	China	117.17	31.90	2015.11.02–2022.12.19	[48]
Xianghe	XH	China	116.96	39.75	2018.06.14–2022.05.31	[45], [49]
Rikubetsu	RJ	Japan	143.77	43.46	2014.06.24–2021.06.30	[50]
Saga	JS	Japan	130.29	33.24	2011.07.28–2022.10.14	[51]
Tsukuba	TK	Japan	140.12	36.05	2014.03.28–2021.03.31	[52]
Anmyeondo	AN	Korea	126.33	36.54	2015.02.02–2018.04.18	[53]

Rikubetsu (RJ), Saga (JS), Tsukuba (TK), and Anmyeondo (AN) (see Fig. 1). Among the six stations, HF and XH are located in China, RJ, JS, and TK are located in Japan, and AN is located in Korea. The observed data with the GGG2020 version were used to validate satellite XCO_2 products. However, since the AN station has not released the GGG2020 version of the data, the GGG2014 version of this station was used [47]. Table II shows the general information of the six stations and the temporal range of selected data.

III. Methods

The remotely sensed XCO_2 products were compared with the TCCON observations to validate their accuracies. The ideal approach to match ground-based data with satellite data is to pair the data between them at the same location and at the same time. However, only a small subset of data pairs meet this criterion. However, satellite sensors and ground sensors have different observation frequencies and spatial extent of sampling, which requires the selection of a suitable spatiotemporal matching method.

To collect sufficient data pairs to carry out robust validation, scholars used relatively looser spatiotemporal matching criteria. Liang et al. [20] chose a spatial and temporal matching range of the satellite data to the station data within a latitude of 2°, longitude of 2.5°, and a time difference within 1 h to screen the GOSAT XCO_2 and OCO-2 XCO_2 data. Meng et al. [23] indicated that the consistency between the NIES-GOSAT XCO_2 and the TCCON data rose with the smaller spatial matching range, adopting a spatial matching of $1° \times 1°$ and a temporal matching range of 1 h. Zhang et al. [19] validated the NIES-GOSAT XCO_2 data using observations from seven TCCON stations in the Northern Hemisphere used spatial matching ranges from 1° to 5° and temporal matching ranges from 1 to 3 h, and the results showed that the consistency between the ground-based and satellite data did not differ much with different spatial and temporal matching ranges. Wunch et al. [22] validated the OCO-2 XCO_2 product by TCCON data using a spatial matching range that latitude and longitude within $\pm 5°$ and $\pm 10°$, respectively, and a temporal matching range of less than 30 min. However, if the number of data pairs was too small (less than 5), the temporal matching range was extended to 2 h.

Referring to previous studies, the following spatiotemporal matching methods are adopted in this study to ensure that sufficient samples are available to provide robust validation conclusions: spatially, the satellite XCO_2 data within $\pm 2°$ latitude and $\pm 2.5°$ longitude boxes centered on the TCCON stations were selected; temporally, TCCON observations within ± 2 h of the satellite overpass time were selected. Satellite XCO_2 data and TCCON XCO_2 data that meet the spatial and temporal requirements are averaged and then subsequently compared. This means that all the remotely sensed XCO_2 of a satellite overpass time within the spatial box were averaged, and all the TCCON observed XCO_2 within the ± 2 h window were also averaged to generate one satellite-TCCON data pair.

Based on the generated data pairs, the mean bias (MB), absolute error (AE), mean absolute error (MAE), and coefficient of determination (R^2) were calculated to quantify the accuracy of the satellite XCO_2 products. The formulas are as follows:

$$\mathrm{MB} = \frac{\sum_{j=1}^{N} (x_j - X_j)}{N} \quad (1)$$

$$\mathrm{AE} = |x_j - X_j| \quad (2)$$

$$\mathrm{MAE} = \frac{\sum_{j=1}^{N} |x_j - X_j|}{N} \quad (3)$$

$$R^2 = 1 - \frac{\sum_{j=1}^{N} (X_i - x_i)^2}{\sum_{j=1}^{N} \left(X_i - \bar{X}\right)^2} \quad (4)$$

where x is the satellite XCO_2, X is the TCCON XCO_2,$\bar{X}$ is the average value of TCCON XCO_2, and N is the number of data pairs.

IV. Results and Discussions

A. Overall Validation Results

The nine satellite retrieval XCO_2 products (ACOS-GOSAT, NIES-GOSAT, BESD-GOSAT, OCFP-GOSAT, SRFP-GOSAT, GOSAT-2, OCO-2, OCO-3, and EMMA) were compared with the observations from six TCCON stations located in East Asia. The AEs of all samples were calculated to draw the box plots of the AE of the nine products (see Fig. 2). The red solid line within each box represents the mean value of AE, and the black dashed line represents the median value of AE. The absolute errors of most satellite XCO_2 products were mainly less than 2 ppm, except for the GOSAT-2 XCO_2 product. Among all the nine products, the OCO-2 XCO_2 product outperformed others, with 50% of the AEs ranging from 0.48 to 1.71 ppm. The ACOS-GOSAT and EMMA XCO_2 products also showed commendable accuracies, with 50% of the AEs ranging from 0.51 to 1.77 ppm and from 0.47 to 1.80 ppm, respectively. The OCO-3 XCO_2 product had a slightly lower stability than previous products, with 50% of the AEs ranging from 0.57 to

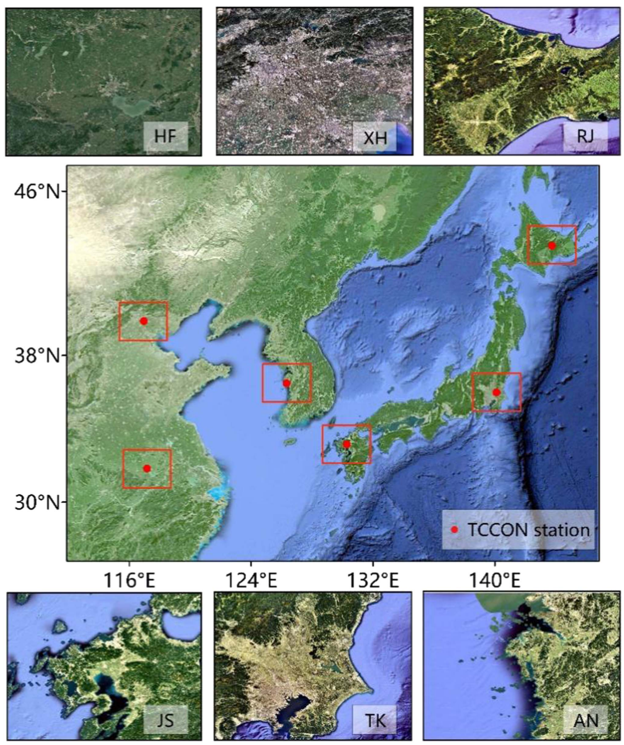

Fig. 1. Locations of six TCCON stations in East Asia (red box is the 2° × 2.5° latitude × longitude box centered at each TCCON station).

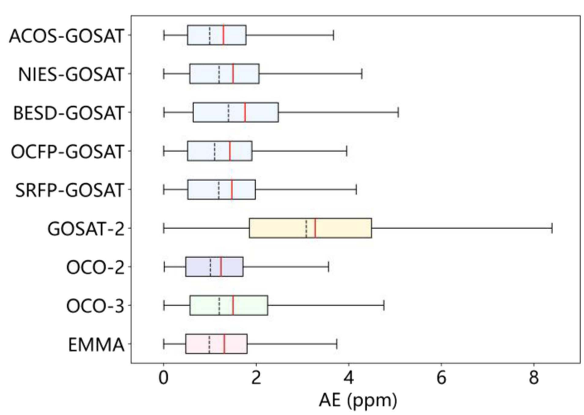

Fig. 2. Box plots of the AE of the nine satellite XCO_2 products. The red solid line within each box represents the mean value of AE, and the black dashed line represents the median value of AE.

2.24 ppm. The GOSAT-2 XCO_2 product showed much poorer accuracy than other products, with 50% of the AEs ranging from 1.85 to 4.49 ppm, suggesting a much lower overall accuracy and also a much higher instability of this bias uncorrected product. In addition, it was noted that the median AEs of all products were lower than the mean values, indicating right-skewed distributions of all the products which generally suggests that there are a lot of extremely high-error samples.

The ACOS-GOSAT XCO_2 product shows the highest accuracy of all XCO_2 products. The OCO-2 XCO_2, OCO-3 XCO_2, and GOSAT-2 XCO_2 products are the only XCO_2 products for these three satellites, respectively. The EMMA XCO_2 product is a typical ensemble XCO_2 product. Therefore, these five products were selected for further validation. Fig. 3 shows the scatter plots between the TCCON observed XCO_2 and the remotely sensed XCO_2 from the OCO-2, ACOS-GOSAT, OCO-3, GOSAT-2, and EMMA products. For the OCO-2 XCO_2, ACOS-GOSAT XCO_2, EMMA XCO_2, and OCO-3 XCO_2 products, most sample points concentrated near the 1:1 line, suggesting good agreements with the TCCON observations. The MAEs of these four XCO_2 products were 1.24, 1.29, 1.31, and 1.50 ppm, respectively. R^2 of these four XCO_2 products were 0.94, 0.93, 0.93, and 0.80, respectively. Moreover, the OCO-2, ACOS, and EMMA products showed no obvious overestimation or underestimation. The OCO-3 product showed a slight overestimation. For the GOSAT-2 product, sample points were generally far from the 1:1 line, showing a large deviation from the TCCON observations, since the GOSAT-2 product is not bias corrected. Moreover, most samples were located above the 1:1 line, indicating a serious overestimation.

The performances of the five typical satellite XCO_2 products at each TCCON station were also validated. Fig. 4 shows the scatter plots between the TCCON observed XCO_2 and the remotely sensed XCO_2 of the OCO-2, ACOS-GOSAT XCO_2, EMMA XCO_2, OCO-3, and GOSAT-2 XCO_2 products at the six TCCON stations, respectively. Due to the relatively short operation period, OCO-3 had no colocation data with the AN station, and GOSAT-2 had no colocation data with the AN station. Therefore, there are just five scatterplots of the OCO-3 and GOSAT-2 XCO_2 products. The OCO-2 XCO_2 product showed good agreement with TCCON XCO_2 at the HF, RJ, JS, and TK stations, with R^2 of 0.94, 0.95, 0.96, and 0.95, and MAE of 1.20, 1.12, 1.08, and 0.95 ppm, respectively. It showed slightly lower accuracy with TCCON XCO_2 at the AN station, with an R^2 of 0.88 and an MAE of 1.03 ppm. At the XH station, it showed the worst agreement with ground-based XCO_2, with an R^2 of 0.76 and an MAE of 1.83 ppm. The ACOS-GOSAT XCO_2 product was in high agreement with the TCCON XCO_2 at the RJ, JS, and TK stations, with R^2 of 0.96, 0.95, and 0.92, respectively, and MAE of 1.58, 1.22, and 1.12 ppm, respectively, but there was an underestimation at the RJ station. The agreement between the ACOS-GOSAT XCO_2 product and the TCCON XCO_2 at the HF, XH, and AN stations was slightly lower than those at the RJ, JS, and TK stations, with R^2 of 0.80, 0.81, 0.81 and MAE of 1.52, 1.46, and 1.26 ppm. The EMMA XCO_2 product had a good agreement with TCCON XCO_2 at RJ, JS, and AN stations, with R^2 of 0.97, 0.95, and 0.93, respectively, and MAE of 1.25, 1.17, and 1.40 ppm, respectively. It had lower agreements with the ground-based XCO_2 at HF and TK stations, with R^2 of 0.85 and 0.88, and MAE of 1.53 and 1.20 ppm, respectively. At the XH station, it showed the worst agreement with ground-based XCO_2, with an R^2 of 0.74 and an MAE of 1.77 ppm. Moreover, there was an overestimation problem, with an ME of 1.11 ppm. The OCO-3 XCO_2 product had good agreement with TCCON XCO_2 at HF, RJ, and JS stations, with R^2 of 0.85, 0.84, and 0.83, and MAE of 1.35, 1.10, and 1.27 ppm, respectively. It had the worst agreement with TCCON XCO_2 at the TK station, with an R^2 of 0.69 and an MAE of 1.06 ppm. At the HF, XH, JS, and TK stations, OCO-3 XCO_2 showed slight overestimations

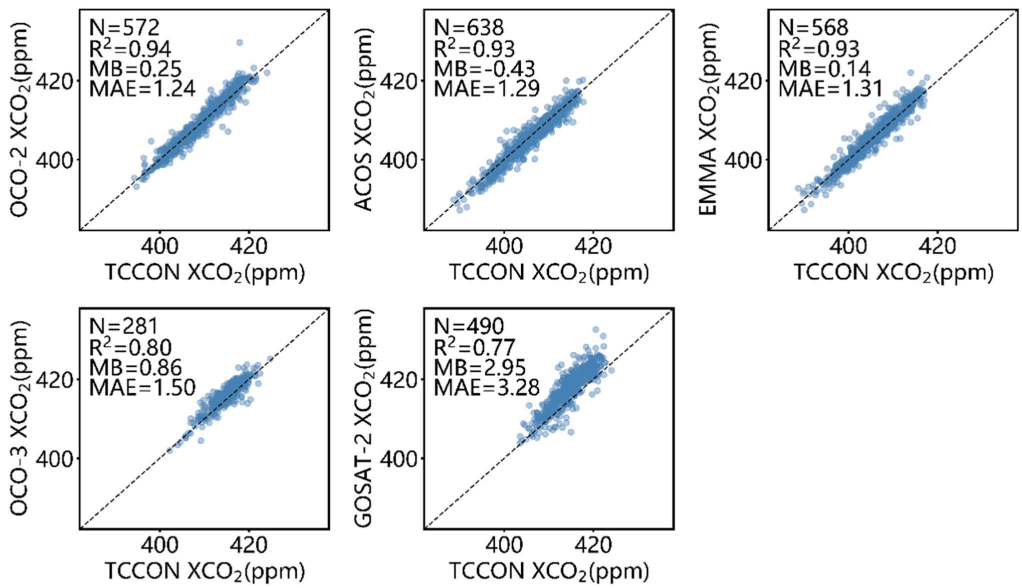

Fig. 3. Scatter plots between the TCCON observed XCO_2 and satellite-derived XCO_2 from the OCO-2, ACOS-GOSAT, OCO-3, GOSAT-2, and EMMA products.

compared with TCCON observations. The GOSAT-2 XCO_2 product showed poor agreements with TCCON XCO_2 at all five stations since the GOSAT-2 XCO_2 product is not bias corrected. Most of the sample points were distributed above the 1:1 line, indicating a significant overestimation. Among the five stations, the highest agreement between GOSAT-2 XCO_2 and TCCON XCO_2 was found at the AN station, with an R^2 of 0.89 and an MAE of 2.47 ppm.

The accuracies of the nine satellite XCO_2 products were also validated over four seasons. Fig. 5 shows the box plots of AEs over four seasons between TCCON observed XCO_2 and remotely sensed XCO_2. Among all the nine products, the ACOS-GOSAT XCO_2, NIES-GOSAT XCO_2, and BESD-GOSAT XCO_2 products showed similar AEs over the four seasons. OCFP-GOSAT XCO_2 and EMMA XCO_2 were slightly lower in accuracy in summer, with 50% of the AEs ranging from 0.64 to 2.23 ppm and from 0.63 to 2.20 ppm, respectively. The SRFP-GOSAT XCO_2, OCO-2 XCO_2, and OCO-3 XCO_2 products had lower accuracy in winter, with 50% of the AEs ranging from 0.61 to 2.32 ppm, 0.57 to 2.02 ppm, and 0.82 to 2.36 ppm, respectively. The OCO-2 XCO_2 products had higher accuracy in spring and the lowest accuracy in winter. The GOSAT-2 XCO_2 product had much worse accuracy than the other products in all four seasons, with 50% of the AEs ranging from 2.98 to 4.89 ppm, 1.66 to 4.30 ppm, 1.36 to 3.97 ppm, and 1.72 to 3.91 ppm, respectively. In general, most of the satellite XCO_2 products showed no obvious difference in accuracy across the four seasons, indicating that the sensors and the retrieval algorithms are less sensitive to the seasonal changes of land and atmospheric properties.

B. Discussion

In recent years, GHG monitoring has attracted increasing attention. Several GHG monitoring satellites have been launched and a lot of XCO_2 products have been developed from these satellite data. However, most of the previous validation studies have focused on one or two satellite XCO_2 products, and there is a lack of comprehensive validation analysis of existing products. Using the observations from six TCCON stations in East Asia, this study proposed a comprehensive validation on nine XCO_2 products retrieved from four major GHG monitoring satellites (GOSAT, GOSAT-2, OCO-2, and OCO-3), which can provide a valuable reference for researchers and users to select proper satellite XCO_2 products, especially in East Asia.

Generally, the OCO-2 XCO_2 product is closer to TCCON observations than other products, with an MAE of 1.24 ppm. The ACOS-GOSAT XCO_2 and EMMA-GOSAT XCO_2 products also show good accuracies, with MAEs of 1.29 and 1.31 ppm, respectively. The NIES-GOSAT XCO_2, BESD-GOSAT XCO_2, OCFP-GOSAT XCO_2, SRFP-GOSAT XCO_2, and OCO-3 XCO_2 products show slightly lower accuracies, with the MAEs higher than 1.5 ppm but lower than 2.0 ppm. The GOSAT-2 XCO_2, which is bias uncorrected, shows much poor accuracy, with an MAE of 3.28 ppm. Liang et al. [20] proposed that OCO-2 XCO_2 product had higher accuracy than the NIES GOSAT product on a global scale, and this article shows that the accuracy of OCO-2 XCO_2 products in East Asia is also higher than that of NIES-GOSAT XCO_2 products. Wunch et al. [22] pointed out that the MAE between OCO-2 XCO_2 products and 19 TCCON globally XCO_2 is less than 0.4 ppm, which is smaller than the MAE in East Asia. The GOSAT-2 XCO_2 estimates are generally much higher than TCCON observations, suggesting a significant overestimation problem. The GOSAT-2 official validation report based on global TCCON sites also indicated that this product had a high error and positive deviation [54], [55], [56].

The accuracy of TCCON XCO_2 at different stations is not consistent with that of satellite retrieval of XCO_2. The RJ, JS, AN, and TK TCCON stations generally showed better agreements between satellite estimates and TCCON observations. Aerosols are the most important factor contributing to errors

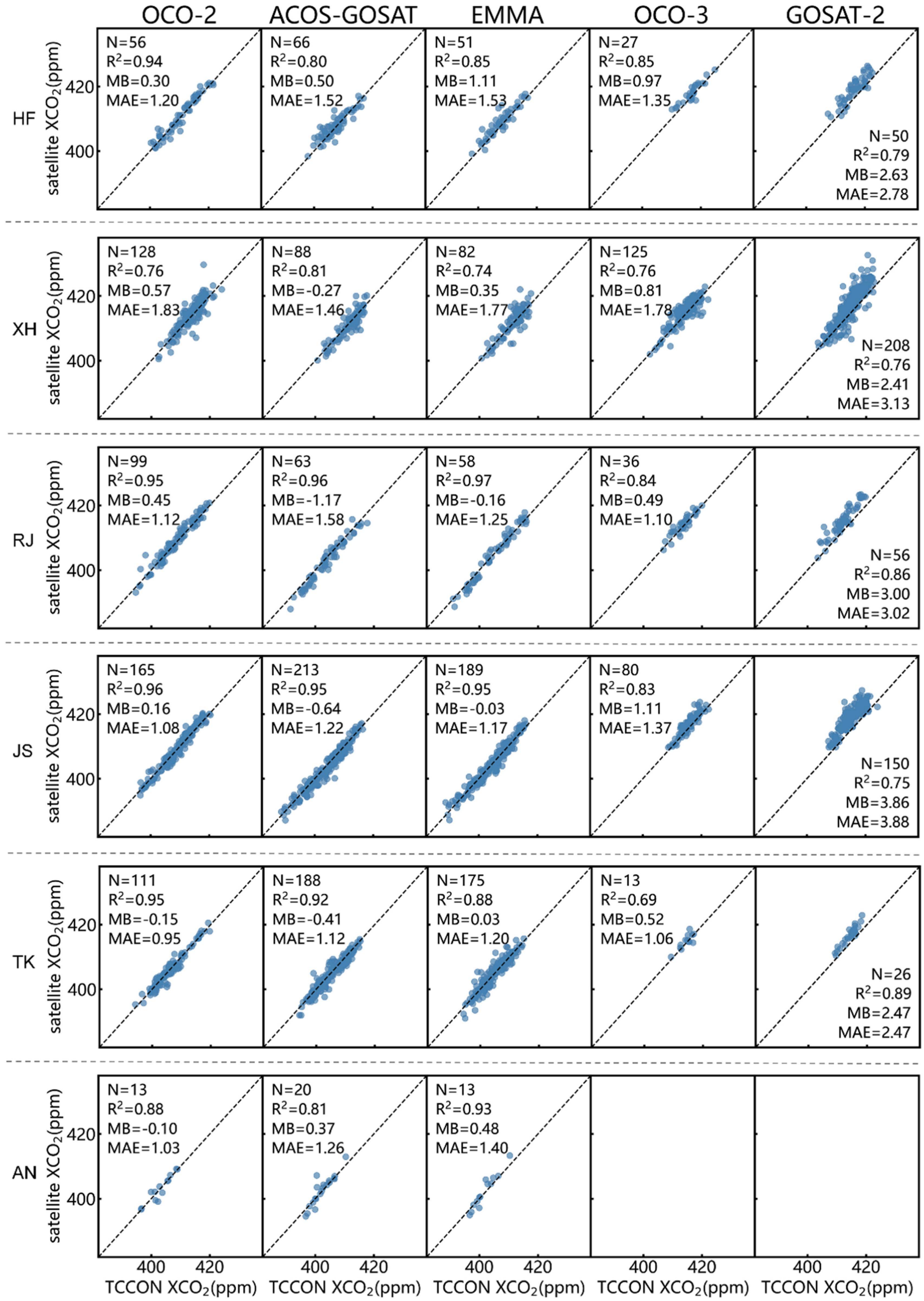

Fig. 4. Scatter plots between the TCCON observed XCO_2 and the satellite-derived XCO_2 from OCO-2 XCO_2, ACOS-GOSAT XCO_2, EMMA XCO_2, OCO-3 XCO_2, and GOSAT-2 XCO_2 products at six TCCON stations.

in satellite-derived XCO_2. Bie et al. [57] pointed out that the uncertainty of satellite-retrieved XCO_2 tends to increase with enlargements of albedo and aerosol optical depth. Connor et al. [58] proposed that although the absolute size of the aerosol error is quite small, it varies considerably from place to place, and the main variable error is caused by the aerosol. In addition, the TCCON observation is the point-scale measurement of XCO_2 but the satellite estimate is the retrieved XCO_2 in a footprint within the $2° \times 2.5°$ latitude $\times$ longitude boxes centered at each TCCON station. The land cover of the TCCON stations and

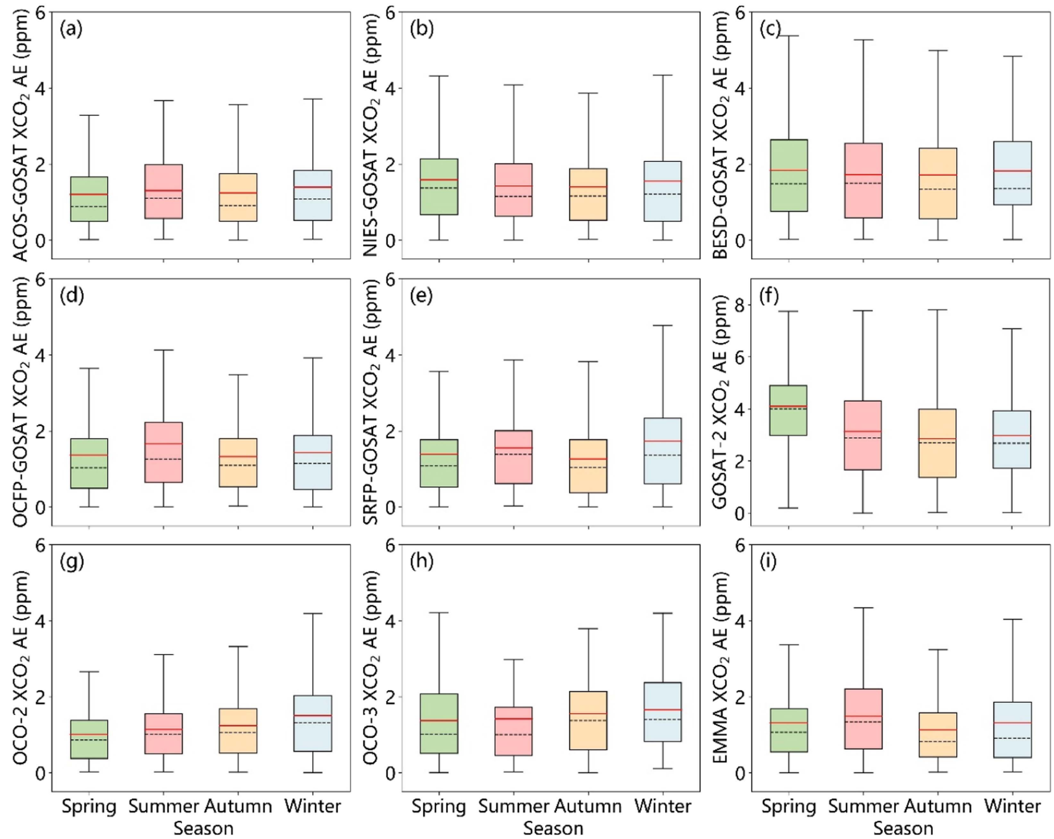

Fig. 5. Box plots of the AEs for nine satellite XCO_2 products over four seasons. The red solid line within each box represents the mean value of AE, and the black dashed line represents the median value of AE.

the remote sensing footprint may differ, which may reduce the consistency between the ground-based and satellite XCO_2 data.

The TCCON observation is the point-scale measurement of XCO_2. However, the satellite estimate is the retrieved XCO_2 in a footprint. Moreover, the satellite estimates within a square box were averaged to compare with TCCON observations for robust validation. The large spatial difference between the TCCON and satellite data will bring uncertainty to the validation. Due to the relatively long period of the satellite data in this study, a relatively small spatial box was able to ensure sufficient samples, which effectively reduced the uncertainty caused by the spatial scale difference. Considering that different TCCON sites have different landscape patterns and spatial heterogeneities, spatial representations of sites need to be studied by high-resolution aircraft observations for determining proper spatial box for collocation with TCCON observations.

In addition to accuracy, other factors need to be taken into account, including spatial resolution, spatial coverage, and temporal period. The spatial resolutions of GOSAT and GOSAT-2 are about 10 km (10.5 and 9.7 km, respectively), whereas the spatial resolutions of OCO-2 and OCO-3 are 2.25 km $\times$ 1.29 km. The OCO-2 and OCO-3 have a much better spatial resolution, providing better spatial details and reducing the influence of cloud contamination. The GOSAT and GOSAT-2 have wide swath widths but sparse footprints (five footprints with an overall more than 900-km swath width), whereas the OCO-2 and OCO-3 have narrow swath widths but relatively denser footprints (eight footprints with an overall 10-km swath width). Therefore, the GOSAT and GOSAT-2 can capture XCO_2 information at a large scale with sparse observation density, and the OCO-2 and OCO-3 can observe XCO_2 at a small scale in a dense manner. In addition, GOSAT has a long temporal coverage ($>$14 years), providing support for monitoring long-term spatiotemporal variations of XCO_2. Therefore, the differences in the spatial resolution, swath width, and temporal coverage should also be considered when selecting satellite XCO_2 products. Considering that different satellite XCO_2 products showed their advantages in different aspects, a feasible multi-product ensemble strategy is also an intelligent choice. Multi-product integration can fully utilize the advantages of different products and effectively improve the spatial and temporal coverage, and also accuracy, especially for the studies of long-term CO_2 variations.

V. Conclusion

Satellite-based remote sensing can observe XCO_2 at large scales, providing vital data support for carbon reduction tasks. However, the accuracies of satellite XCO_2 products vary with XCO_2 sensors and retrieval algorithms. It is important to provide a comprehensive validation of the existing satellite XCO_2 product. In this study, nine satellite retrieval XCO_2 products

(ACOS-GOSAT, NIES-GOSAT, BESD-GOSAT, OCFP-GOSAT, SRFP-GOSAT, GOSAT-2, OCO-2, OCO-3, and EMMA) were validated by comparing with the observations from six TCCON stations situated in East Asia. Different products exhibited quite different performances. The OCO-2 XCO_2 product achieved the highest accuracy, followed by the ACOS-GOSAT XCO_2 and EMMA XCO_2 products. The GOSAT-2 XCO_2 product had poor accuracy since it is bias uncorrected and is not recommended for applications before bias correction. However, empirical bias corrected coefficients, which are provided by Yoshida et al. [39], should be applied to the GOSAT-2 XCO_2 product (v02.00 data). This study can serve as a valuable reference for researchers and government agencies in selecting XCO_2 data, providing critical data support for carbon emission reduction.

ACKNOWLEDGMENT

The authors would like to thank TCCON Science Team for providing TCCON observations, NASA for providing the ACOS-GOSAT, OCO-2, and OCO-3 XCO_2 products, NIES for providing the NIES-GOSAT and GOSAT-2 XCO_2 products, the University of Bremen for providing BESD-GOSAT and EMMA XCO_2 products, the University of Leicester for providing OCFP-GOSAT XCO_2 product, and The Netherlands Institute for Space Research for providing SRFP-GOSAT XCO_2 product. The authors would like to thank David Pollard of the National Institute of Water and Atmospheric Research for his kind help on TCCON data. The TCCON data were obtained from the TCCON Data Archive hosted by CaltechDATA at https://tccondata.org.

REFERENCES

[1] J. Timperley, "What can the world learn from New Zealand on climate?," *Lancet Planet. Health*, vol. 4, no. 5, pp. E176–E177, May 2020, doi: 10.1016/S2542-5196(20)30109-1.

[2] Y. Xu and G. Cui, "Influence of spectral characteristics of the Earth's surface radiation on the greenhouse effect: Principles and mechanisms," *Atmos. Environ.*, vol. 244, Jan. 2021, Art. no. 117908, doi: 10.1016/j.atmosenv.2020.117908.

[3] W. Gao et al., "Industrial carbon dioxide capture and utilization: State of the Art and future challenges," *Chem. Soc. Rev.*, vol. 49, no. 23, pp. 8584–8686, Dec. 2020, doi: 10.1039/D0CS00025F.

[4] A. A. Lacis, G. A. Schmidt, D. Rind, and R. A. Ruedy, "Atmospheric CO_2: Principal control knob governing Earth's temperature," *Science*, vol. 330, no. 6002, pp. 356–359, Oct. 2010, doi: 10.1126/science.1190653.

[5] S. A. Sejas, P. C. Taylor, and M. Cai, "Unmasking the negative greenhouse effect over the Antarctic Plateau," *npj Climate Atmos. Sci.*, vol. 1, no. 1, Jul. 2018, Art. no. 17, doi: 10.1038/s41612-018-0031-y.

[6] H. Rodhe, "A comparison of the contribution of various gases to the greenhouse effect," *Science*, vol. 248, no. 4960, pp. 1217–1219, Jun. 1990, doi: 10.1126/science.248.4960.1217.

[7] A. Kuze et al., "Examining partial-column density retrieval of lower-tropospheric CO_2 from GOSAT target observations over global megacities," *Remote Sens. Environ.*, vol. 273, May 2022, Art. no. 112966, doi: 10.1016/j.rse.2022.112966.

[8] A. Demirbas, "Correlations between carbon dioxide emissions and carbon contents of fuels," *Energy Sources, B, Econ., Planning, Policy*, vol. 1, no. 4, pp. 421–427, Dec. 2006, doi: 10.1080/15567240500402628.

[9] H. Grassl, "Climate change challenges," *Surv. Geophys.*, vol. 32, no. 4/5, pp. 319–328, Sep. 2011, doi: 10.1007/s10712-011-9129-z.

[10] J. H. Hashim and Z. Hashim, "Climate change, extreme weather events, and Human health implications in the Asia Pacific Region," *Asia-Pac. J. Public Health*, vol. 28, no. 2 Suppl, pp. 8S–14S, Mar. 2016, doi: 10.1177/1010539515599030.

[11] M. Mengel, A. Nauels, J. Rogelj, and C.-F. Schleussner, "Committed sea-level rise under the Paris Agreement and the legacy of delayed mitigation action," *Nature Commun.*, vol. 9, no. 1, Feb. 2018, Art. no. 601, doi: 10.1038/s41467-018-02985-8.

[12] H. S. Baker et al., "Higher CO_2 concentrations increase extreme event risk in a 1.5°C world," *Nature Climate Change*, vol. 8, no. 7, pp. 604–608, Jul. 2018, doi: 10.1038/s41558-018-0190-1.

[13] K. Zickfeld, A. H. MacDougall, and H. D. Matthews, "On the proportionality between global temperature change and cumulative CO_2 emissions during periods of net negative CO_2 emissions," *Environ. Res. Lett.*, vol. 11, no. 5, May 2016, Art. no. 055006, doi: 10.1088/1748-9326/11/5/055006.

[14] D. Satterthwaite, "How urban societies can adapt to resource shortage and climate change," *Philos. Trans. Roy. Soc. A*, vol. 369, no. 1942, pp. 1762–1783, May 2011, doi: 10.1098/rsta.2010.0350.

[15] C. Mora et al., "Broad threat to humanity from cumulative climate hazards intensified by greenhouse gas emissions," *Nature Climate Change*, vol. 8, no. 12, pp. 1062–1071, Dec. 2018, doi: 10.1038/s41558-018-0315-6.

[16] M. Kiel et al., "Urban-focused satellite CO_2 observations from the Orbiting Carbon Observatory-3: A first look at the Los Angeles megacity," *Remote Sens. Environ.*, vol. 258, Mar. 2021, Art. no. 112314, doi: 10.1016/j.rse.2021.112314.

[17] A. G. Hu, "China's achievement of peak carbon targets by 2030 and major pathways," *J. Beijing Inst. Technol. (Social Sci. Ed.)*, vol. 21, no. 3, pp. 1–15, May 2021, doi: 10.12120/bjutskxb202103001.

[18] B. Y. Yu et al., "Research on China's Co_2 emission pathways under the carbon neutral target," *J. Beijing Inst. Technol. (Social Sci. Ed.)*, vol. 23, no. 2, pp. 17–24, 2021, doi: 10.15918/j.jbitss1009-3370.2021.7380.

[19] M. Zhang, X. Y. Zhang, and R. X. Liu, "Study on the validation of atmospheric CO_2 from satellite hyper spectral remote sensing," *Prog. Climate Change Res.*, vol. 10, no. 6, pp. 427–432, Nov. 2014, doi: 10.3969/j.issn.1673-1719.2014.06.005.

[20] A. Liang, W. Gong, G. Han, and C. Xiang, "Comparison of satellite-observed XCO_2 from GOSAT, OCO-2, and ground-based TCCON," *Remote Sens.*, vol. 9, no. 10, Oct. 2017, Art. no. 1033, doi: 10.3390/rs9101033.

[21] S. Zhang, Y. Bai, X. He, H. Huang, Q. Zhu, and F. Gong, "Comparisons of OCO-2 satellite derived XCO_2 with *in situ* and modeled data over global ocean," *Acta Oceanologica Sinica*, vol. 40, no. 4, pp. 136–142, Apr. 2021, doi: 10.1007/s13131-021-1844-9.

[22] D. Wunch et al., "Comparisons of the Orbiting Carbon Observatory-2 (OCO-2) XCO_2 measurements with TCCON," *Atmos. Meas. Techn.*, vol. 10, no. 6, pp. 2209–2238, Jun. 2017, doi: 10.5194/amt-10-2209-2017.

[23] X. Y. Meng et al., "Validation and analysis of GOSAT XCO_2 measurements by TCCON sites," *Meteorol. Phenomena*, vol. 44, no. 10, pp. 1306–1317, Oct. 2018, doi: 10.7519/j.issn.1000-0526.2018.10.007.

[24] J. Fang et al., "Global evaluation and intercomparison of XCO_2 retrievals from GOSAT, OCO-2, and TANSAT with TCCON," *Remote Sens.*, vol. 15, Oct. 2023, Art. no. 5073, doi: 10.3390/rs15205073.

[25] J. Zheng, H. Zhang, and S. Zhang, "Comparison of atmospheric carbon dioxide concentrations based on GOSAT, OCO-2 observations and ground-based TCCON data," *Remote Sens.*, vol. 15, Oct. 2023, Art. no. 5172, doi: 10.3390/rs15215172.

[26] S. Karbasi, H. Malakooti, M. Rahnama, and M. Azadi, "Study of mid-latitude retrieval XCO_2 greenhouse gas: Validation of satellite-based shortwave infrared spectroscopy with ground-based TCCON observations," *Sci. Total Environ.*, vol. 836, Aug. 2022, Art. no. 155513, doi: 10.1016/j.scitotenv.2022.155513.

[27] A. Kuze, H. Suto, M. Nakajima, and T. Hamazaki, "Thermal and near infrared sensor for carbon observation Fourier-transform spectrometer on the Greenhouse Gases Observing Satellite for greenhouse gases monitoring," *Appl. Opt.*, vol. 48, no. 35, pp. 6716–6733, Dec. 2009, doi: 10.1364/AO.48.006716.

[28] J. Hong et al., "Potential improvement of XCO_2 retrieval of the OCO-2 by having aerosol information from the A-train satellites," *GIScience Remote Sens.*, vol. 60, no. 1, May 2023, Art. no. 209968, doi: 10.1080/15481603.2023.2209968.

[29] S. Chen et al., "Optimization of the OCO-2 cloud screening algorithm and evaluation against MODIS and TCCON measurements over land surfaces in Europe and Japan," *Adv. Atmos. Sci.*, vol. 37, no. 4, pp. 387–398, Apr. 2020, doi: 10.1007/s00376-020-9160-4.

[30] L. Mandrake, C. Frankenberg, C. W. O'Dell, G. Osterman, P. Wennberg, and D. Wunch, "Semi-autonomous sounding selection for OCO-2," *Atmos. Meas. Techn.*, vol. 6, no. 10, pp. 2851–2864, Oct. 2013, doi: 10.5194/amt-6-2851-2013.

[31] B. Dils et al., "The Greenhouse Gas Climate Change Initiative (GHG-CCI): Comparative validation of GHG-CCI SCIAMACHY/ENVISAT and TANSO-FTS/GOSAT CO_2 and CH_4 retrieval algorithm products with measurements from the TCCON," *Atmos. Meas. Techn.*, vol. 7, no. 6, pp. 1723–1744, Jun. 2014, doi: 10.5194/amt-7-1723-2014.

[32] M. Reuter et al., "Retrieval of atmospheric CO_2 with enhanced accuracy and precision from SCIAMACHY: Validation with FTS measurements and comparison with model results," *J. Geophys. Res.*, vol. 116, Feb. 2011, Art. no. D4301, doi: 10.1029/2010JD015047.

[33] D. Yang et al., "Toward high precision XCO_2 retrievals from TanSat observations: Retrieval improvement and validation against TCCON measurements," *J. Geophys. Res., Atmos.*, vol. 125, no. 22, 2020, Art. no. e2020JD032794, doi: 10.1029/2020JD032794.

[34] A. Butz, O. P. Hasekamp, C. Frankenberg, and I. Aben, "Retrievals of atmospheric CO_2 from simulated space-borne measurements of backscattered near-infrared sunlight: Accounting for aerosol effects," *Appl. Opt.*, vol. 48, no. 18, pp. 3322–3336, Jun. 2009, doi: 10.1364/AO.48.003322.

[35] L. Wu et al., "XCO_2 observations using satellite measurements with moderate spectral resolution: Investigation using GOSAT and OCO-2 measurements," *Atmos. Meas. Techn.*, vol. 13, no. 2, pp. 713–729, Feb. 2020, doi: 10.5194/amt-13-713-2020.

[36] Y. Jung et al., "Impact of aerosol property on the accuracy of a CO_2 retrieval algorithm from satellite remote sensing," *Remote Sens.*, vol. 8, no. 4, Apr. 2016, Art. no. 322, doi: 10.3390/rs8040322.

[37] H. Suto et al., "Thermal and near-infrared sensor for carbon observation Fourier transform spectrometer-2 (TANSO-FTS-2) on the Greenhouse gases observing SATellite-2 (GOSAT-2) during its first year in orbit," *Atmos. Meas. Techn.*, vol. 14, no. 3, pp. 2013–2039, Mar. 2021, doi: 10.5194/amt-14-2013-2021.

[38] Y. Oishi, T. Y. Nakajima, and T. Matsunaga, "Difference between forward- and backward-looking bands of GOSAT-2 CAI-2 cloud discrimination used with Terra MISR data," *Int. J. Remote Sens.*, vol. 37, no. 5, pp. 1115–1126, Mar. 2016, doi: 10.1080/2150704X.2016.1145822.

[39] Y. Yoshida et al., "Quality evaluation of the column-averaged dry air mole fractions of carbon dioxide and methane observed by GOSAT and GOSAT-2," *SOLA*, vol. 19, pp. 173–184, 2023, doi: 10.2151/sola.2023-023.

[40] Y. Bi, Q. Wang, Z. Yang, J. Chen, and W. Bai, "Validation of column-averaged dry-air mole fraction of CO_2 retrieved from OCO-2 using ground-based FTS measurements," *J. Meteorol. Res.*, vol. 32, no. 3, pp. 433–443, Jun. 2018, doi: 10.1007/s13351-018-7118-6.

[41] C. Jin et al., "A long-term global XCO_2 dataset: Ensemble of satellite products," *Atmos. Res.*, vol. 279, Dec. 2022, Art. no. 106385, doi: 10.1016/j.atmosres.2022.106385.

[42] M. Reuter et al., "A joint effort to deliver satellite retrieved atmospheric CO_2 concentrations for surface flux inversions: The ensemble median algorithm EMMA," *Atmos. Chem. Phys.*, vol. 13, no. 4, pp. 1771–1780, Feb. 2013, doi: 10.5194/acp-13-1771-2013.

[43] D. Wunch et al., "The Total Carbon Column Observing Network," *Philosoph. Trans. Roy. Soc. A.*, vol. 369, no. 1943, pp. 2087–2112, May 2011, doi: 10.1098/rsta.2010.0240.

[44] C. Liu et al., "Long-term observations of atmospheric constituents at the first ground-based high-resolution Fourier-transform spectrometry observation station in China," *Engineering*, vol. 22, pp. 201–214, Mar. 2023, doi: 10.1016/j.eng.2021.11.022.

[45] Y. Yang et al., "New ground-based Fourier-transform near-infrared solar absorption measurements of XCO_2, XCH_4 and XCO at Xianghe, China," *Earth Syst. Sci. Data*, vol. 12, no. 3, pp. 1679–1696, Jul. 2020, doi: 10.5194/essd-12-1679-2020.

[46] Y.-S. Oh et al., "Characteristics of greenhouse gas concentrations derived from ground-based FTS spectra at Anmyeondo, South Korea," *Atmos. Meas. Techn.*, vol. 11, no. 4, pp. 2361–2374, Apr. 2018, doi: 10.5194/amt-11-2361-2018.

[47] J. L. Laughner et al., "The Total Carbon Column Observing Network's GGG2020 data version," *Earth Syst. Sci. Data*, to be published, 2023, doi: 10.5194/essd-2023-331.

[48] C. Liu, W. Wang, and Y. Sun, "TCCON data from Hefei(PRC), Release GGG2020.R1," CaltechDATA, Nov. 2023. https://doi.org/10.14291/tccon.ggg2020.hefei01.R1

[49] M. Zhou, P. Wang, N. Kumps, C. Hermans, and W. Nan, "TCCON data from Xianghe, China, Release GGG2020.R0," CaltechDATA, Sep. 2022. https://doi.org/10.14291/tccon.ggg2020.xianghe01.R0

[50] I. Morino, H. Ohyama, A. Hori, and H. Ikegami, "TCCON data from Rikubetsu (JP), Release GGG2022.R0," CaltechDATA, Sep. 20, 2022. https://doi.org/10.14291/tccon.ggg2020.rikubetsu01.R0

[51] S. Kawakami et al., "TCCON data from Saga (JP), Release GGG2020.R0," CaltechDATA, Sep. 2022. https://doi.org/10.14291/tccon.ggg2020.saga01.R0

[52] I. Morino, H. Ohyama, A. Hori, and H. Ikegami, "TCCON data from Tsukuba (JP), 125HR, Release GGG2020.R0," CaltechDATA, Sep. 2022. https://doi.org/10.14291/tccon.ggg2020.tsukuba02.R0

[53] T.-Y. Goo, Y.-S. Oh, and V. A. Velazco, "TCCON data from Anmeyondo (KR), release GGG2014.R0," CaltechDATA, Oct. 2014. [Online]. Available: https://data.caltech.edu/records/266

[54] NIES GOSAT-2 Project, "Summary of the validation on GOSAT-2 TANSO-FTS-2 SWIR L2 column-averaged dry-air mole fraction product," Nov. 2022.

[55] NIES GOSAT-2 Project, "Summary of the validation on GOSAT-2 TANSO-FTS-2 SWIR L2 column-averaged dry-air mole fraction product (Ver. 01.04)," Nov. 2022.

[56] M. Buchwitz et al., "GOSAT-2 quality assessment summary," Nov. 2022.

[57] N. Bie et al., "Regional uncertainty of GOSAT XCO_2 retrievals in China: Quantification and attribution," *Atmos. Meas. Techn.*, vol. 11, no. 3, pp. 1251–1272, Mar. 2018, doi: 10.5194/amt-11-1251-2018.

[58] B. Connor et al., "Quantification of uncertainties in OCO-2 measurements of XCO_2: Simulations and linear error analysis," *Atmos. Meas. Techn.*, vol. 9, no. 10, pp. 5227–5238, Oct. 2016, doi: 10.5194/amt-9-5227-2016.

Meng Ji received the B.S. degree in remote sensing science and technology in 2021 from the Nanjing University of Information Science and Technology, Nanjing, China, where she is currently working toward the M.S. degree in 3S integration and meteorological applications with the School of Remote Sensing and Mapping Engineering.

Her research interests include thermal infrared remote sensing, environmental remote sensing, and nighttime light remote sensing.

Yongming Xu received the M.S. degree in cartography and geographical information systems from the Institute of Remote Sensing Applications, Chinese Academy of Sciences, Beijing, China, in 2005, and the Ph.D. degree in remote sensing of resource and environment from the Nanjing University, Nanjing, China, in 2010.

He is currently a Professor with the School of Remote Sensing and Geomatics Engineering, Nanjing University of Information Science and Technology, Nanjing, China. His research interests include thermal infrared remote sensing, environmental remote sensing, and nighttime light remote sensing.

Yang Zhang received the B.S. degree in remote sensing science and technology in 2021 from the Nanjing University of Information Science and Technology, Nanjing, China, where she is currently working toward the M.S. degree in 3S integration and meteorological applications with the School of Remote Sensing and Mapping Engineering.

Her current research focuses on environmental remote sensing.

Yaping Mo received the M.S. degree in 3S integration and meteorological applications from the Nanjing University of Information Science and Technology, Nanjing, China, in 2023. She is currently working toward the Ph.D. degree in geography with the School of the Environment, Geography and Geosciences, University of Portsmouth, Portsmouth, U.K.

Her research interests include climate change, thermal infrared remote sensing, and environmental remote sensing.

Shanyou Zhu received the M.S. degree in mineral resource prospecting and exploration from the Shandong University of Science and Technology, Tai'an, China, in 2003, and the Ph.D. degree in electromagnetic field and microwave technology from the Shanghai Institute of Technical Physics, Chinese Academy of Sciences, Shanghai, China, in 2006.

He is currently a Professor with the Nanjing University of Information Science and Technology, Nanjing, China. His research interests include the basic theory and application of thermal infrared remote sensing and environmental remote sensing.

Wei Wang received the M.S. degree in optics from Sichuan University, Chengdu, China, in 2005, and the Ph.D. degree in optics from the University of Science and Technology of China, Hefei, China, in 2013.

She is currently a researcher fellow with the Hefei Institutes of Physical Science, Chinese Academy of Science, Hefei, China. Her research interests include infrared spectroscopy, environmental optics and technique, and ground-based remote sensing.

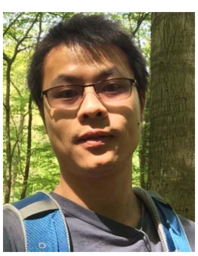

Minqiang Zhou received the Ph.D. degree in atmospheric science from the Institute of Atmospheric Physics, Chinese Academy of Sciences, Beijing, China, in 2017.

From 2015 to 2021, he was a Scientist SW11 in the Royal Belgian Institute for Space 90 Aeronomy (BIRA-IASB), Brussels, Belgium. He is currently an Associate Professor with the Institute of Atmospheric Physics, Chinese Academy of Sciences, Beijing, China. His research interests include ground-based and satellite infrared remote sensing,

Isamu Morino received the Doctor of Science degree in astronomical science from The Graduate University for Advanced Studies, SOKENDAI, Hayama, Japan, in 1996.

He is currently the Head of the Satellite Remote Sensing Section and validation team lead in Satellite Observation Center, Earth System Division, National Institute for Environmental Studies (NIES), Tsukuba, Japan.

He is responsible for the validation of GOSAT and GOSAT-2 data. His research interests include the validation and applications of greenhouse gas satellites.

Hirofumi Ohyama received the D.Sc. degree in earth and planetary system sciences from Kobe University, Kobe, Japan, in 2009.

He is currently a senior researcher with the National Institute for Environmental Studies, Tsukuba, Japan, and is involved in the GOSAT Series project. His research interests include remote sensing of atmospheric trace gases from ground-based and space-based spectroscopic observations.

Kei Shiomi received the Doctor of Science degree in earth and planetary science from the University of Tokyo, Tokyo, Japan, in 2001.

He was with the Remote Sensing Technology Center of Japan for AMSR and AMSR-E data analysis. He is currently with the Earth Observation Research Center, Japan Aerospace Exploration Agency, Tsukuba, Japan, where he is in charge of GOSAT and GOSAT-2 calibration and data processing. His research interests include atmospheric remote sensing by space-based and ground-based instruments.

Young-Suk Oh received the Ph.D. degree in electric engineering from Hanyang University, Seoul, South Korea, in 2020.

He is currently a research scientist with the Innovative Meteorological Research Department, National Institute of Meteorological Sciences, Seogwipo, South Korea. His research interests include the observation and analysis of greenhouse gases.